Vacuum ultraviolet photoionization mass spectrometric study of C_{60}

R. K. Yoo, B. Ruscic, and J. Berkowitz

Chemistry Division, Argonne National Laboratory, Argonne, Illinois 60439

Gaseous C_{60} has been studied by photoionization mass spectrometry between the ionization threshold and 40.8 eV. An adiabatic threshold of 7.57 ± 0.01 eV is observed, which may be slightly low due to hot bands. The energy derivative of the photoion yield curve is in rough agreement with the He I photoelectron spectrum on the positions of some peaks, but others are weak or absent. The discrepancy is not attributed to autoionization, but rather to selection rules governing the ejection of low energy electrons into high angular momentum waves. $C_{60}^{+}{}^{+}$ is observed at higher energies, and becomes ~ 0.6 as intense as C_{60}^{+} at 40.8 eV. The photoion yield curve of $C_{60}^{+}{}^{+}$, approximately linear well above threshold, appears to exhibit curvature near threshold, thwarting an attempt to make a distinction between two alternative values of the second ionization potential. Fragmentation to form C_{58}^{+} is only observed at the highest energy, 40.8 eV. The unimolecular decay is modelled by quasiequilibrium theory. In this model, the kinetic shift is of the order of 30 eV, and the minimum energy for dissociation into $C_{58}^{+} + C_{2}$ seems to be 6.0–6.5 eV.

I. INTRODUCTION

Buckminsterfullerene, C_{60}, has attracted enormous interest because of its apparently exceptional stability, very high symmetry and other properties, some of which may have important practical application. From the viewpoint of photoionization mass spectrometry, it offers the opportunity to study a very large molecule in the gas phase, testing our understanding of ionization and unimolecular decay at limits not previously available. With the discovery[1] of a method for producing C_{60} and its larger fullerene analogs in gram quantities, it has become possible to study the photoionization and photodissociation of these molecules in a more controlled fashion.

Earlier studies,[2] utilizing the C_{60}^{+} cation directly generated by a vaporization laser and then photodissociated by another laser at either 4.9 eV (KrF) or 6.4 eV (ArF) concluded "that the first fragments of C_{60}^{+} are detected only after absorption of at least three photons of ArF radiation (and possibly more)," at an observation time of 3 μs. The fragments consisted of even numbered clusters, i.e., C_{58}^{+}, C_{56}^{+}, etc. This was contrasted with the fragmentation of smaller C_{n}^{+} clusters (up to C_{31}^{+}), which tended to lose C_{3} units.[3] The photofragmentation of C_{60}^{+} induced by 6.4 eV photons at a fluence of 15 mJ cm^{-2} produced even numbered fragments down to at least C_{36}^{+}, with a maximum at C_{50}^{+}. Such large fragmentations caused O'Brien et al.[2] to have doubts as to whether "...sequential (C_{2}) loss is reasonable for the very high order fragmentations. Single event C_{e} loss where e is an even number > 2 deserves consideration as well."

More recently, Radi, et al.[4] generated C_{60}^{+} and other ions by "laser desorption from a graphite rod," and accelerated them to 8 keV. The ions were mass selected by passing through a magnetic field, and then entered a 1 m field free region. Those C_{60}^{+} ions undergoing unimolecular decay in the field free region to $C_{58}^{+} + C_{2}$ were subsequently energy analyzed in a high resolution electrostatic sector. The kinetic energy distribution of C_{58}^{+} was converted into a center-of-mass kinetic energy release distribution, which had a maximum at ≈ 0.2 eV and a long high energy tail. Statistical phase space theory was used to model this kinetic energy release distribution. The calculations depended most strongly upon the C_{58}^{+}–C_{2} binding energy and the internal energy in the metastable C_{60}^{+} parent ion. Using internal energy and the C_{2}-binding energy as variable parameters which had to simultaneously fit the kinetic energy distribution, the absolute rate constant and the C_{2} vs C_{4} loss branching ratio, they deduced that the average internal energy of the decomposing C_{60}^{+} was 39 eV, while the C_{2} binding energy was 4.6 eV. This was roughly consistent with the conclusion of O'Brien, et al.[2] that at least $3 \times 6.4 = 19.2$ eV of internal energy in C_{60}^{+} was necessary for observable fragmentation. Both studies had difficulty in rationalizing C_{2} loss from C_{60}^{+} "...though C_{3} is the most abundant species in the equilibrium vapor (above graphite) and the most stable low mass fragment.[4]" O'Brien, et al.[2] favored a four-center transition state. Radi, et al.[4] argued that this mechanism implied a substantial reverse activation energy, but their phase space calculations suggested a statistical decay mechanism with negligible reverse activation energy and relatively weak bonds between C_{2} and C_{58}^{+}. Neither study appears to have considered the relative stability of the combined systems ($C_{57}^{+} + C_{3}$) and ($C_{58}^{+} + C_{2}$), rather than just the relative stabilities of C_{2} and C_{3}.

Luffer and Schram[5] obtained the 70 eV electron impact mass spectrum of C_{60}. Here, C_{60} vapor was produced by sublimation from a C_{60} sample prepared by the method of Ref. 1. The mass spectrum was dominated by C_{60}^{+}, with about 7% of C_{58}^{+}, and successively smaller abundances with larger C_{2n} loss, down to C_{44}^{+} at 0.2%. By contrast to the low abundance of fragment ions, $C_{60}^{+}{}^{+}$ was 2/3 as intense as C_{60}^{+}, and even $C_{60}^{+}{}^{+}{}^{+}$ was observed, about 4% of C_{60}^{+}. An-

other surprising feature was the collision-induced dissociation (CID) of $C_{60}^{+\ +}$, which did not reveal decomposition into two singly-charged units, but rather into $C_{58}^{+\ +} + C_2$, $C_{56}^{+\ +} + C_2 ...$ to $C_{40}^{+\ +} + C_2$.[5,6] (A much weaker signal of singly-charged fragments than doubly charged fragments was recently reported[7] in the CID of $C_{60}^{+\ +}$, but this was attributed to formation of excited $C_{60}^{+\ +}$ by electron capture, and its subsequent dissociation.)

The observation that double ionization far exceeds fragmentation may seem surprising at first glance. For small molecules, Coulomb repulsion reduces the abundance of doubly charged ions to the level of roughly 1%, whereas fragment ion abundances are comparable to parent ions at 70 eV.[8] However, earlier 70 eV electron impact studies,[9,10] on large conjugated hydrocarbons (naphthalene, anthracene, and 4-ring compounds) already displayed ratios of doubly to singly charged abundances ranging from ~0.12–0.18, comparable to fragment:parent ratios. The larger hydrocarbons can evidently maintain larger charge separation, reducing the tendency toward Coulomb explosion. This tendency apparently continues from the C_{18} hydrocarbons to C_{60}.

The 70 eV electron impact mass spectrum has some relationship to a photoionization mass spectrum. If the Born approximation were valid, the 70 eV electron beam could be considered to be equivalent to photon beams spanning the energy range from the ionization potential to 70 eV, and weighted by $1/E$. The first ionization potential of C_{60} seems fairly well established. A value of 7.61 ± 0.11 eV was obtained by charge transfer bracketing in a Fourier transform ICR cell,[11] and UV photoelectron spectroscopic studies on thin films of C_{60} yielded a vertical ionization energy estimated to be 7.6 ± 0.2 eV.[12] More recently, a gas phase photoelectron spectrum gave 7.61 ± 0.02 eV.[13] However, there is a discrepancy in values reported for the second ionization potential. McElvany et al.[14] using charge transfer bracketing in a Fourier transform ICR mass spectrometer, obtained 9.7 ± 0.2 eV as the energy to ionize C_{60}^{+}, whereas Lifshitz[15] et al. measured the translational energy loss in the charge-stripping reaction

$$C_{60}^{+} + M \rightarrow C_{60}^{+\ +} + M + e$$
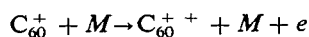
and deduced 12.25 ± 0.5 eV for this quantity. Both the first and second ionization potentials of C_{60} have been calculated by Rosen and Wästberg,[16] using the local density approximation. They obtained 6.9 and 7.8 eV for the first ionization potential (IP), using respectively the $X\alpha$ exchange-correlation potential with $\alpha = 0.7$ and the parametrization of von Barth and Hedin.[17] This was reported before an accurate IP had been determined experimentally. For the second IP (i.e., the IP of C_{60}^{+}), they obtained 10.1 eV ($\alpha = 0.7$) and 10.8 eV (von Barth and Hedin). Hence, the calculation of the second IP falls between the two experimental values, favoring the lower one.

In summary, previous studies indicate that photoionization of C_{60} should have an onset at 7.6 eV, fragmentation to C_{58}^{+} should not be detectable before 26.8 eV and possibly 46 eV, and $C_{60}^{+\ +}$ should have an onset at either 17.3 ($\pm$ 0.2) or 19.85 ($\pm$ 0.5) eV.

II. EXPERIMENTAL ARRANGEMENT

An early version of our vacuum ultraviolet (VUV) photoionization mass spectrometer was rejuvenated for these experiments. It consists of a 1 m normal incidence VUV monochromator mated to a 60° sector magnetic mass spectrometer. With 4 kV accelerating potential, the mass spectrometer can be used to access m/e values in excess of 720 (C_{60}^{+}). Three different types of light sources were utilized: the hydrogen many-line spectrum from ~1640 to ~970 Å, the Hopfield continuum of helium from ~1000 to ~600 Å, and line sources of He II and Ne II from 584 to 304 Å. For the latter, a grating blazed at 290 Å was used, whereas for the H_2 and He continuum sources a 1200 l/mm, 800 Å blazed grating was employed. The mass spectrometer slits were widened for high transmission, but could still easily resolve one C unit at $m/e = 720$. The wavelength resolution was varied between 0.83–2.5 Å (FWHM) between 1640 – 600 Å. Below 600 Å, resolution was not a factor with the line sources used. The light intensity was monitored by the photoelectric current produced on a polished Ni surface. The wavelength response of this photodetector had previously been determined between 580–1660 Å. It was extrapolated to 300 Å, using the measurement of Cairns and Samson.[18]

Fullerene soot was prepared in an electric arc system similar to that described by Kratschmer et al.[1] The fullerenes were extracted by toluene. After drying, the sample was loaded into a Mo oven. The oven was radiatively heated by a zigzag tungsten filament, which in turn was surrounded by radiation shields. A water cooled shield kept the vacuum chamber at a tolerable temperature. An additional electrode atop this structure could be used to prevent electrons from the filament entering the ionization chamber. With this arrangement, the background ion count was of the order of 1/min. The temperature of the oven was measured with a Pt, Pt 10% Rh thermocouple.

III. EXPERIMENTAL RESULTS

At a typical measurement temperature (~600 °C), the ratio of $m/e = 840$ (C_{70}^{+}) to $m/e = 720$ (C_{60}^{+}) was about 0.12 at 584 Å. All subsequent experiments were performed on C_{60}^{+} or lower masses. The only lower masses at which photoion signals were observed with $\lambda \geqslant 460$ Å were $m/e = 720$ (C_{60}^{+}) and $m/e = 360$ ($C_{60}^{+\ +}$). An attempt was made to observe $m/e = 696$ (C_{58}^{+}) and $m/e = 672$ (C_{56}^{+}) at 460 Å where the light intensity was relatively strong. No net photoion signal was observed at either mass; the fragment to parent ion ratio was determined to be $\leqslant 1/350$ at C_{58}^{+}. However, at 304 Å some significant signal was observed at C_{58}^{+}, and possibly C_{56}^{+}. In 5 min of counting time, we observed 12 counts of C_{58}^{+}, of which 5 counts was attributed to background (monitored at a nearby wavelength off the peak). For C_{56}^{+}, the corresponding counts were 9 and 5. A weak $C_{60}^{+\ +}$ signal was observed at the very intense Ne resonance lines (composite of 735.8962 and 743.7195 Å, about 16.84 eV) and initially thought to represent a near threshold value for $C_{60}^{+\ +}$. However, a similar low level signal at the same mass was observed at the equally intense Lyman α (1215.67
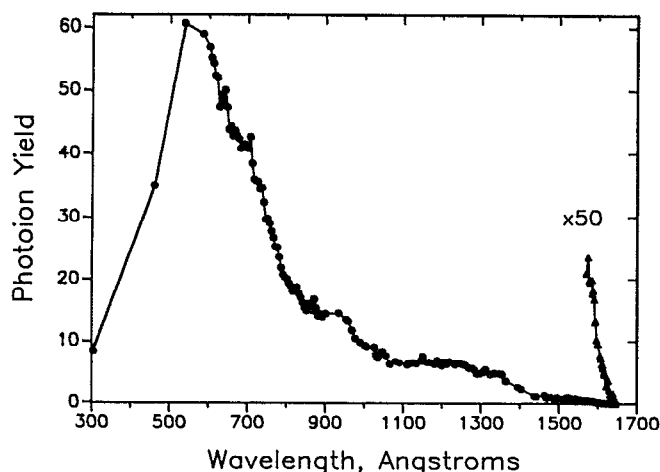
FIG. 1. Photoion yield curve of C_{60}^+ (C_{60}) from threshold to 304 Å, with magnified threshold region.

Å $\equiv$ 10.20 eV) and Lyman β (1025.72 Å $\equiv$ 12.09 eV) lines, and consequently attributed to a secondary process. Most likely, it results from photoelectrons formed at the photodetector (near ground potential) accelerated into the ionization chamber (at + 4 kV). This low level signal was only encountered with the very intense lines, and was treated as a light dependent background.

A. The photoion yield curve of C_{60}^+ (C_{60})

The normalized ion yield curve between threshold and 304 Å is shown in Fig. 1. The approach to threshold (see expanded scale) is very nearly linear. The apparent threshold occurs at 1638 $\pm$ 2 Å $\equiv$ 7.57 $\pm$ 0.01 eV. This is about 0.04 eV lower than the value obtained by photoelectron spectroscopy. A possible interpretation is that the current value corresponds to the adiabatic IP, whereas the PES value is a vertical IP. However, the influence of temperature must be considered. At 800 K, close to the experimental temperature, the average vibrational internal energy is an astonishing 4.6 eV $\equiv$ 106.5 kcal/mol! This is based on the calculated frequencies of C_{60} given by Stanton and Newton.[19] Most of these normal modes should remain inactive spectators in the direct photoionization transition, and hence their internal energies should not be available. Only the totally symmetric modes should be Franck–Condon active, and there are two of these with calculated frequencies of 610 and 1667 cm^{-1}. If the geometrical structure of C_{60}^+ is identical to that of C_{60}, then the $1 \to 1$, $2 \to 2$, etc. transitions fall directly on the $0 \to 0$ transitions; the adiabatic and vertical ionization potentials are the same, and hot bands do not contribute. This must be very nearly the case here, since a $1 \to 0$ transition of the 1667 cm^{-1} mode would cause a displacement between vertical and adiabatic IP of 0.2 eV (much larger than observed) and even for the 610 cm^{-1} mode, the 1–0 transition would cause a shift of 0.076 eV.

The photoion yield appears to increase more than linearly between $\sim$ 1500–1350 Å. Between ca. 1300–1100 Å, the ion yield is nearly flat. As one proceeds to shorter wavelengths, the photoion yield again increases, displaying a

rounded step between 1000–850 Å, and then a sharper increase to $\sim$ 584 Å. Shortly thereafter, the photoion yield descends rapidly. At 304 Å, the relative photoionization cross section is about 1/7 that at $\sim$ 540 Å.

B. The photoion yield curve of C_{60}^{++}

The weak intensity of C_{60}^{++} limited our studies to a few lines: He II (303.78 Å), Ne II (460.73–462.39 Å), He I$_\beta$ (537.03 Å), He I$_\alpha$ (584.33 Å) and Ne I (626.82–629.74 Å). As mentioned earlier, a weak signal due to a second order process was observed at Ne I (735.90–743.72 Å). The photoion yield curve of C_{60}^{++} (C_{60}) is shown in Fig. 2. Between 537–304 Å, the growth is roughly linear. At 584 Å, there is still a significant C_{60}^{++} intensity, but it is only $\sim$ 1/230 that of C_{60}^+. At $\sim$ 628 Å, the C_{60}^{++} signal is comparable to the uncertainty of measurement. There does seem to be significant curvature as this curve approaches threshold. A rough extrapolation yields an apparent threshold of $\sim$ 635 Å $\equiv$ 19.5 eV, which implies a second ionization potential ($C_{60}^+ \to C_{60}^{++}$) of $\sim$ 11.9 eV, close to the value given by Lifshitz et al.[15] (12.25 $\pm$ 0.5 eV). However, there is no fundamental basis for this extrapolation, and enhanced curvature near threshold could readily accommodate the lower value. The C_{60}^{++}/C_{60}^+ intensity ratio at 304 Å is about 0.6.

IV. INTERPRETATION OF RESULTS

A. C_{60}^+

An idealized direct photoionization process would consist of a succession of step functions, each succeeding step corresponding to a new (higher) state of the ion being accessed. If we limit ourselves to the electronic ground state of the ion, there could be a progression of vibrational steps, corresponding to Franck–Condon active vibrational excitation. The Franck–Condon active vibrations should be totally symmetric, and should reflect the change in geometry between the neutral species and its cation. If there is no significant change in geometry, one should expect an abrupt step. This is contrary to the present observation, which displays a roughly linear growth with excess energy. This could be accommodated within the framework of direct ionization if we
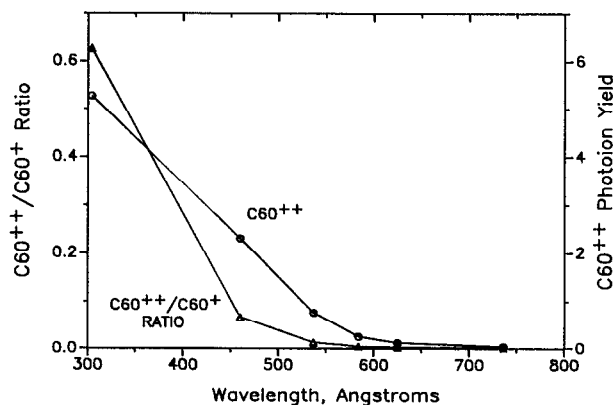

FIG. 2. Photoion yield curve of C_{60}^{++} (C_{60}). The ordinate is relative to that in Fig. 1.
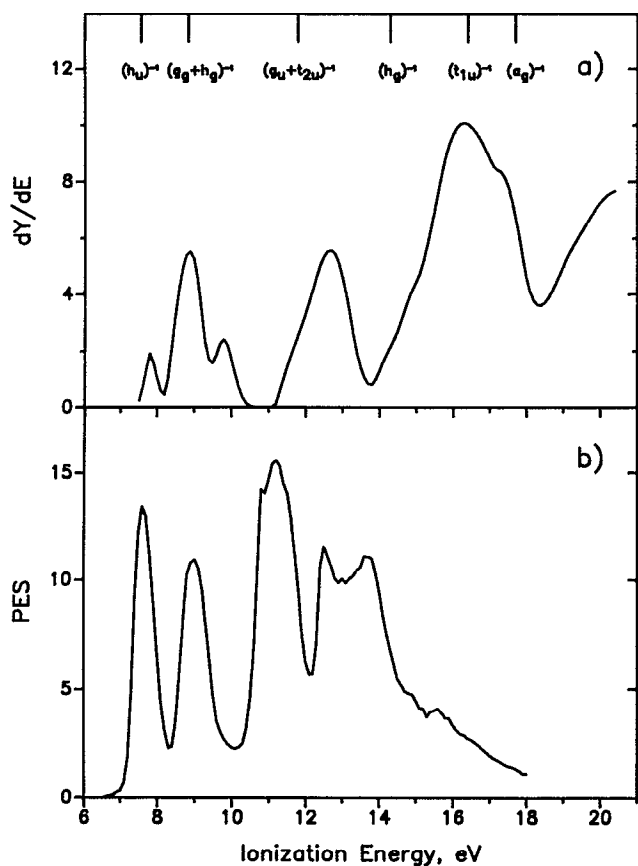
FIG. 3. (a) The energy derivative of the photoion yield of C_{60}^+, as a function of photon energy. The assignment is based on orbital energies (denoted by vertical bars on top) calculated by S. Larsson, A. Volosov, and A. Rosen, Chem. Phys. Lett. **137**, 501 (1987). (b) He I photoelectron spectrum of C_{60} (from Ref. 12).

visualize a series of small vibrational steps (a staircase), which would appear linear with poor resolution or inherent broadening.

The derivative with respect to photon energy of the photoion yield curve provides a test of the relative importance of direct vs indirect (or auto-) ionization. If direct ionization is dominant, peaks should appear in the derivative function at about the same position as in a photoelectron spectrum. In Fig. 3(a), we display such a derivative, obtained from a smoothed fit to the photoion yield curve. This can be compared with a He I photoelectron spectrum,[12] shown in Fig. 3(b). There is fairly good agreement in peak position between Fig. 3(a) and the first, second, fourth, and perhaps 6th peaks in the photoelectron spectrum. The third and fifth peaks are missing in Fig. 3(a), and the first peak is exceptionally small. However, there do not appear to be spurious, or extra peaks in the derivative curve which could have been introduced by autoionization.

If direct ionization is dominant, why are the relative intensities of Fig. 3(a) so different from those of Fig. 3(b)? Weaver et al.[20] recently obtained photoemission spectra of C_{60} in the condensed phase at several higher energies. They already noted that the relative intensity (I_1/I_2) of the first two peaks changed from 0.88 at $h\nu = 40$ eV to 1.48 at 45 eV. These first two bands also have different relative intensities

at He I (21.2 eV) and He II (40.8 eV) in the photoelectron spectrum of Lichtenberger et al.[12] In our derivative spectrum [Fig. 3(a)], the first, third, and fifth bands are weak or absent, while the second, fourth, and sixth bands are strong. Haddon et al.[21] have calculated the successive orbital energies of the highest occupied molecular orbitals (HOMO'S) of C_{60}. They display an alternation in parity, from h_u (uppermost occupied) to $(g_g + h_g)$, $(g_u + t_{2u})$, h_g, t_{1u}, and a_g. Weaver et al.[20] have already noted that the variation in their I_1/I_2 intensity ratios could be due to the odd and even symmetry of these states. The variation in intensities between Figs. 3(a) and 3(b) is more extreme. In the following discussion, we present a possible explanation for this behavior.

Haddon et al.[21] have shown the relationship of the uppermost occupied orbitals, expressed in icosahedral symmetry, and their parentage in spherical symmetry. Thus, for example, an A_g orbital transforms like an s orbital ($L = 0$), a t_{1u} in icosahedral symmetry is like a p-orbital ($L = 1$), and an h_g orbital behaves likes a d orbital ($L = 2$). It turns out that the HOMOs, in descending order, correspond to $L = 5,4,3,2,1$, with alternating odd and even character.

The ground state of C_{60} is ^1A_g. Hence, according to selection rules, the electric dipole allowed upper states must have T_{1u} symmetry. This includes the ionized (cation + photoelectron) states. By Koopmans' theorem arguments, the ground state of C_{60}^+ should be ^2H_u. The direct product of $H_u \times T_{1u}$ is $t_{1g} + t_{2g} + g_g + h_g$. (The capital letters refer to the symmetry of the cation state or the combined state, the lower-case letters to the photoelectron wave.) Thus, the departing electron must be gerade, and expressed in the spherical group can have either d, g, or i symmetry. The strength of this transition near threshold may be suppressed on two counts.

(1) An $l = 5$ electron may have difficulty becoming an $l = 2$ outgoing wave, since the single electron selection rule is usually $\Delta l = \pm 1$. This problem would not exist for g_g ($l = 4$) or i_g ($l = 6$) outgoing waves.

(2) The departing electron experiences an angular momentum barrier, due to the centrifugal term $l(l + 1)/r^2$ in the potential. Such a barrier is absent or insignificant for s or p outgoing waves; it starts to get significant for d waves, and becomes increasingly important for higher l waves. The effect of the barrier is to depress the ionization probability for very low energy electrons. At higher energies, the photoelectrons can surmount the barrier, but the possibility of interferences between the allowed outgoing waves exists. For g or i outgoing waves, the barrier suppression near the threshold should be very significant.

The first excited state of the cation should be ^2G_g and/or ^2H_g. The imposition of the same dipole rules forces the outgoing photoelectron to have f or h character (^2G_g) and p, f or h character (^2H_g). The p outgoing wave should not experience an angular momentum barrier (though there may be some weakening of the matrix element for an $h \rightarrow p$ transition). The f outgoing wave will experience some threshold suppression, but the $g \rightarrow f$ matrix element is favorable. Taken together, photoemission from this second combined band should be stronger than the first band. Similar arguments can be made for the third and fourth bands. For the fifth and

TABLE I. Symmetry of the departing photoelectron wave upon electron ejection from the various HOMO (in descending order of binding).

Cation state[a]	L^b	$\epsilon_k(I_h)^c$	$\epsilon_k(K)^d$	Observed threshold strength[e]
^2H_u	5	$t_{1g} + h_g + t_{2g} + g_g$	d, g, i	w
^2G_g	4	$t_{2u} + g_u + h_u$	f, h	s
^2H_g		$t_{1u} + h_u + t_{2u} + g_u$	p, f, h	
$^2T_{2u}$	3	$g_g + h_g$	d, g, i	w
^2G_u		$t_{2g} + g_g + h_g$	d, g, i	
^2H_g	2	$t_{1u} + h_u + t_{2u} + g_u$	p, h, f	s
$^2T_{1u}$	1	$a_g + t_{1g} + h_g$	s, d, g, i	w?
^2A_g	0	Ct_{1u}	p	s?

[a] Since each of the MO in C$_{60}$ is fully occupied, the symmetry of each cation state is the symmetry of the molecular orbital from which the electron is ejected.
[b] See also Haddon et al., Ref. 21.
[c] Refers to the symmetry of the outgoing wave in icosahedral symmetry.
[d] Refers to the symmetry of the outgoing wave in spherical symmetry.
[e] From Fig. 3(a).

sixth bands, the states of the cation should be $^2T_{1u}$ and ^2A_g, respectively. Lower l outgoing waves are now possible. In particular, formation of ^2A_g should correspond uniquely with outgoing p waves, which should be strong near threshold. These deliberations are summarized in Table I.

To be sure, autoionization should also be occurring. The delayed ionization in C$_{60}$ and C$_{70}$ observed by Campbell et al.[22] is probably a manifestation of slow autoionization. It is difficult to partition the direct and autoionization contributions from the available information. In particular, the derivative function in Fig. 3(a) does not reveal additional structure which can readily be attributed to autoionization. The symmetry requirements for electronic autoionization are not very restrictive in the present case.

B. C$_{60}^{++}$

The idealized direct double photoionization of a system should exhibit a linear or near-linear increase in photoion yield above threshold.[23] Even for an atom, this behavior is to be expected only for a unique state of the doubly ionized species. If there are additional low lying states, each might be expected to have linear post-threshold behavior. The summation of linear segments would than be similar to direct electron impact single ionization forming successive ionic states. Such a summation of linear segments could look like a quadratic, or higher power law dependence upon excess energy.

We have seen (Fig. 2) that the photoion yield for C$_{60}^{++}$ appears to be linear at higher energies, but may approach threshold with higher curvature. If this is the case, an impact method such as that employed by Lifshitz et al.[15] may be sensitive to the more steeply rising probability. In addition, the time scale of the measurement may influence the threshold value obtained. The ICR measurement of McElvany et al.[14] involves a relatively long time scale. By contrast, the collision stripping of C$_{60}^+$ to C$_{60}^{++}$ measured by Lifshitz et

al.[15] involves a short time scale. This may account for the different double ionization thresholds arrived at by these groups. In this picture, the adiabatic double ionization threshold is ~ 17.3 eV, and the photoion yield curve of C$_{60}^{++}$ may be quite curved near threshold. Additional support for this tentative conclusion is found in a recent paper by Cox et al.[24] These authors state: "Appearance potential (AP) studies on C$_{60}$ suggest that the second IP of C$_{60}$ (and C$_{70}$) is less than 18 eV", with a reference to Hsu and Cox.

Our observed intensity ratio (C$_{60}^{++}$/C$_{60}^+$) is only 0.065 at 26.95 eV, but becomes about 10 times larger at 40.8 eV. The region between these two line sources corresponds to the ejection of electrons from 2s-like orbitals. Such states have been observed in C$_{60}$ in the condensed phase by extreme ultraviolet and x-ray photoelectron spectroscopy.[20] They gain intensity, relative to ionization from 2p-like orbitals, as the photon energy increases. Coincidentally, the 70 eV electron impact spectrum[5] displays a C$_{60}^{++}$/C$_{60}^+$ ratio which is approximately the same as our observation at $h\nu = 40.8$ eV.

C. Fragmentation: C$_{60}^+ \rightarrow$ C$_{58}^+$ + C$_2$

In the present experiment, this fragmentation process was not observed at 26.95 eV, where we were able to establish a limit: C$_{58}^+$/C$_{60}^+ \leqslant 1/350$. At 40.8 eV, with considerable struggle, this ratio was observed to be 0.07 ± 0.04. In addition, a marginal result, $\leqslant 0.04 \pm 0.04$, was obtained for C$_{56}^+$/C$_{60}^+$. Below, we examine the parameters of quasiequilibrium theory to see if they are consistent with this limit.

A preliminary calculation which is essential is to determine the average internal energy of the molecular ion, since this energy is available to the process of unimolecular decay.[25] The vibrational frequencies of C$_{60}$ have been calculated by Stanton and Newton.[19] The accuracy of these calculations has been tested by Bethune et al.,[26] who have obtained experimental values for the four infrared active frequencies and the ten Raman active frequencies. The agreement is sur-

prisingly good for the low frequency modes ($\sim$270–770 cm^{-1}). For the higher frequency modes ($\sim$1100–1575 cm^{-1}) the calculated values are about 170–200 cm^{-1} too high. Consequently, the calculated frequencies appear to be quite reasonable, and if anything, slightly high. Thus, our calculated vibrational energy will be slightly underestimated. Using the frequencies of Stanton and Newton, we compute a vibrational energy of C_{60} amounting to $\sim$10.1 kcal/mol (0.44 eV) at 298 °K, and a whopping 133.0 kcal/mol (5.77 eV) at an approximate experimental temperature of $\sim$900 °K. The rotational energy at 900 °K is 2.7 kcal/mol, probably within the uncertainty of the vibrational calculation. Furthermore, one can raise questions about the availability of the rotational energy for decomposition in this huge molecule, and hence we shall ignore this contribution. If the vibrational internal energy is available, then the total energy in the molecular ion at $h\nu = 26.95$ eV (on the average) is $26.95 - 7.6 + 5.77 = 25.12$ eV. The minimum energy necessary for the dissociation process

$$C_{60}^+ \rightarrow C_{58}^+ + C_2$$
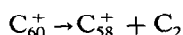
has been estimated by Radi et al.[4] to be 4.6 eV, by fitting statistical phase space theory to their kinetic energy release measurements.

For comparison, the dissociation process

$$C_6H_6^+ \rightarrow C_4H_4^+ + C_2H_2$$

has about the same dissociation energy.[27] In this latter process, benzene cation has the equivalent of nine nominally single C–C bonds, $C_4H_4^+$ (believed to be methylene cyclopropene) effectively six C–C bonds, and acetylene nominally three C–C bonds. Hence, there is no net loss of bond order. However, the resonance energy of $C_6H_6^+$ is about 30 kcal/mol,[28] the strain energy of the three-membered cyclopropene ring is about 28 kcal/mol,[28] and C_2H_2 lacks about 33 kcal/mol for equivalence to three single C–C bonds, which amounts to $\sim$91 kcal/mol, or about 4 eV endothermicity. (These simple calculations ignore the variable strength of the C–H bonds). In the decomposition of C_{60}^+, we have effectively $(60\times4)/2 = 120$ C–C single bonds, 116 for C_{58}^+ and 2 for C_2, a net loss of two C–C bonds, or about 7.6 eV. This kind of comparison led Radi et al.[4] to conclude that there were "relatively weak bonds between the dimer unit and the parent cluster."

Below, we shall compute the rate of unimolecular decay of C_{60}^+ by the microcanonical RRKM expression[29]

$$k(E) = \frac{\alpha G^*(E - E_0)}{hN(E)},$$

where $k(E)$ is the unimolecular decay rate, α is the reaction path degeneracy. $G^*(E - E_0)$ is the number of states of the activated complex, and $N(E)$ is the density of states, with $E_0 \approx 4.6$ eV as a trial value.

To compute G^* and N, we have used Haarhoff's approximation,[30] utilizing the neutral C_{60} frequencies from Stanton and Newton.[19] As one test of the accuracy of our counting of states, we have computed the vibrational energy distribution $[N(E)e^{-E/kT} \text{ vs } E]$ at 900 °K. The result, shown in Fig. 4, is an almost symmetrical distribution with a maximum very
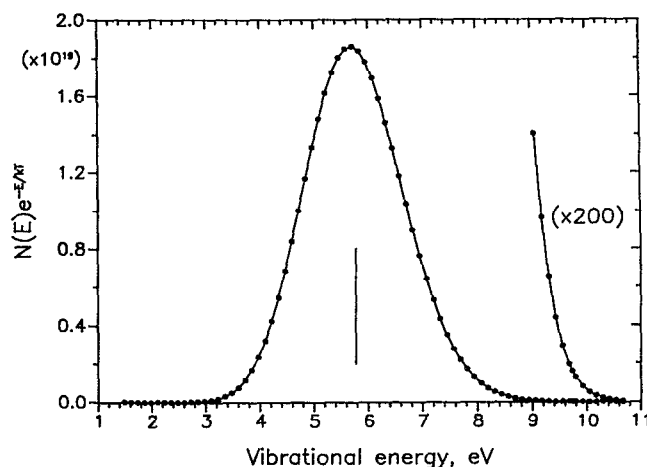

FIG. 4. Vibrational energy distribution of gaseous C_{60} at 900 °K. The vertical line denotes the average vibrational internal energy.

near to the average internal energy (shown as a vertical line). We have compared a direct count (after bunching the 174 vibrations into 11 groups) with Haarhoff's approximation up to $\sim$9000 cm^{-1}, at which energy the direct count is only about 1.4 times higher. We have also used the Beyer–Swinehart algorithm,[31] (with all 174 frequencies) which is essentially a much more efficient direct count. At $E = 25\,000$ cm^{-1}, this procedure yields a count higher by a factor of 1.02 and a density higher by a factor of 1.03 than the Haarhoff method. At the much higher energies which we shall explore here, the difference between a direct count and that from Haarhoff's approximation should be negligible.

In the following calculation, we assume that the vibrational frequencies of C_{60}^+ are the same as those used for C_{60}, and hence $N(E)$ measured above their respective zero point energies will be identical. The transition state will have one frequency less than the C_{60}^+, but most of the 173 frequencies are assumed to be unchanged. To estimate the changes, we assume that each C removed from C_{60}^+ takes away one stretching and two bending frequencies. We also assume a 4-center transition state, with one C–C stretch and 4 bending frequencies. Thus, to zeroth order, we drop a stretching frequency from C_{60}^+ as an estimate for the frequencies of the transition state. Baer et al.[32] chose 966 cm^{-1} as the C–C stretch reaction coordinate in the $C_6H_6^+ \rightarrow C_4H_4^+$ C_2H_2 reaction. In our zeroth order approximation for C_{60}^+ decomposition, we have removed the highest frequency (1722 cm^{-1}) or alternatively, the lowest bending frequency (263 cm^{-1}). We assume that these widely differing frequencies will span the possible sum-of-states of the activated complex. The reaction path degeneracy (α) depends upon which C_2 unit is removed from C_{60}^+. There are 60 C–C bonds which involve a common hexagon–pentagon edge, and 30 C–C bonds which have a common hexagon–hexagon edge. The resulting C_{58}^+ looks more symmetric in the latter case, and hence we choose $\alpha = 30$. The results of the calculations are summarized in Table II and Fig. 5.

The density of states $N(E)$ and the number of states of

TABLE II. Calculated density of states $N(E)$, number of activated complex states $G^*(E - E_0)$ and unimolecular decay rate of C_{60}^+ (900 °K) as a function of photon energy ($\alpha = 30$, trial $E_0 = 4.6$ eV). The numbers in parentheses in the $N(E)$, $G(E - E_0)$ and $k(E)$ columns are powers of 10.

$h\nu$, eV	E, eV	$E - E_0$, eV	$N(E)/cm^{-1}$	$G^*(E - E_0)^a$	$G^*(E - E_0)^b$	$k(E)$ s^{-1a}	$k(E)$ s^{-1b}
15.0	13.2	8.6	1.4(83)	5.6(67)	1.8(68)	3.6(-4)	1.1(-3)
20.0	18.2	13.6	2.6(98)	9.5(86)	3.5(87)	3.3(0)	1.2(1)
25.0	23.2	18.6	9.0(110)	9.3(101)	3.7(102)	9.3(2)	3.7(3)
30.0	28.2	23.6	3.2(121)	1.5(114)	6.6(114)	4.3(4)	1.8(5)
35.0	33.2	28.6	6.7(130)	5.6(124)	2.5(125)	7.5(5)	3.4(6)
40.0	38.2	33.6	1.3(139)	9.3(133)	4.4(134)	6.8(6)	3.2(7)
45.0	43.2	38.6	2.7(146)	1.2(142)	5.6(142)	3.8(7)	1.9(8)
50.0	48.2	43.6	1.6(153)	2.8(149)	1.4(150)	1.6(8)	7.9(8)
55.0	53.2	48.6	2.4(159)	1.4(156)	7.2(156)	5.2(8)	2.7(9)

[a]Frequencies of transition state taken to be those of C_{60}^+, minus the lowest frequency (263 cm^{-1}).
[b]Frequencies of transition state taken to be those of C_{60}^+, minus the highest frequency (1722 cm^{-1}).

the activated complex $G^*(E - E_0)$ are both immense. The rate constant $k(E)$ is approximately two orders of magnitude larger than that calculated by Radi et al.,[4] i.e., ours fall in the measurable range ($\sim 10^4$/s) with an internal energy of ~ 26 eV, while theirs occurs at $\sim 39 \pm 2$ eV.[4] The range of rate constants spanned by the two alternative dropped frequencies is about a factor 4.

Bakowics and Thiel[33] have also calculated C₆₀ vibrational frequencies using MNDO, and obtain almost exactly the same values as Stanton and Newton.[19] Bakowics and Thiel state that these calculated frequencies should be scaled by 0.88 to come closer to experiment. This is roughly what we had previously found (Sec. IV C) by comparing the MNDO calculation of Stanton and Newton[19] with experimental[26] infrared and Raman spectra. Therefore, we also

FIG. 5. The calculated rate constant $k(E)$ vs E for the decomposition $C_{60}^+ \rightarrow C_{58}^+ + C_2$, assuming a "hard" or "soft" transition state, and $E_0 = 4.6$ eV.

calculated $G^*(E - E_0)$ and $N(E)$ by the Haarhoff method scaling each calculated frequency by 0.9. Although $G^*(E - E_0)$ and $N(E)$ increase by 6–7 orders of magnitude, the calculated rate constants decrease by only a factor 1.2–1.4, much less than the spread between alternative transition states.

In the current experiment, the residence time (τ) of C_{60}^+ in the ionization cell is about 11–12 μs. This is also the approximate time the parent ion spends in the field-free region between electrostatic acceleration and magnetic deflection. Consequently, the integrated intensity of C_{58}^+ fragment ion and the metastable ion ($C_{60}^+ \rightarrow C_{58}^+ + C_2$ in field-free region) should be about the same. The latter should appear at $m/e = 672.8$ amu and hence is indistinguishable within our mass resolution from C_{56}^+.

From Fig. 5, we obtain $k(E) \sim 10^7$/s at $h\nu = 40.8$ eV. After a residence time τ, the ratio of dissociated to undissociated ions is $e^{k\tau} - 1$. Thus, essentially all of the C_{60}^+ would be decomposed, if this rate calculation were valid. One may argue that the C_{60}^+ observed at 304 Å ≡ 40.8 eV has a range of internal energies, many of them too low to permit of dissociation. However, we have seen that the ratio of C_{60}^{++} to C_{60}^+ is about 0.6 at = 40.8 eV, and that this ratio has grown by a factor 10 in a span of ~ 14 eV. Hence, a substantial fraction of the ionization at 40.8 eV must be to states with high internal energy. In order that the calculation represented in Fig. 5 and Table II match the observation of C_{58}^+ at 40.8 eV, it would require that only $\sim 7\%$ of the C_{60}^+ states had the required high internal energy.

If, however, we increase E_0 (the minimum energy required for dissociation) to between 6.0–6.5 eV from 4.6 eV, the calculated rate constant is shifted into the experimental domain ($\sim 10^4$/s) for the alternative assumptions regarding the frequencies of the activated complex. With such a value for E_0, the ratio of dissociated to undissociated molecular ions at 460 Å ≡ 26.95 eV is less than 10^{-5}, which is consistent with our upper limit ($\leqslant 1/350$). We tentatively conclude that the QET model employed here, together with our experimental data, argue for an increased value of E_0, which seems plausible based on the aforementioned bond order arguments. The marginal detection of "C_{56}^+" is consistent with the expected metastable peak at "$C_{56.07}^+$."
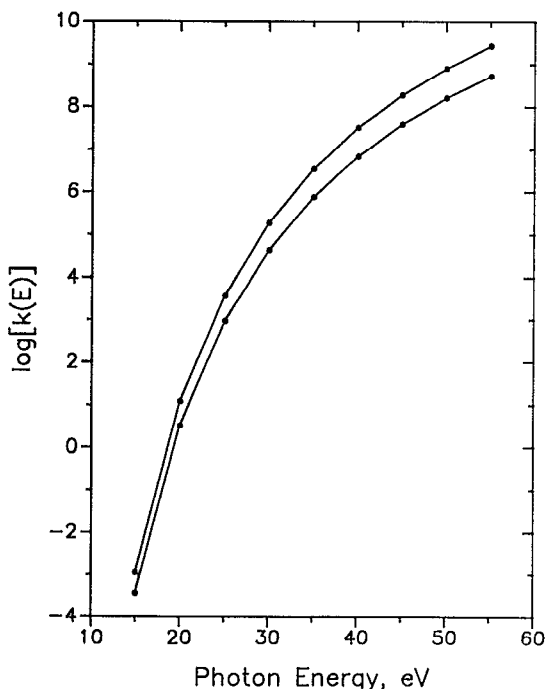
V. CONCLUSIONS

A. Formation of C$_{60}^{+}$

(1) The threshold for photoionization occurs at 7.57 $\pm$ 0.01 eV. Within the uncertainty due to hot bands, this is consistent with the photoelectron spectroscopic value 7.61 $\pm$ 0.02 eV.

(2) The energy derivative of the photoion yield curve displays some peaks corresponding to those observed in the He I photoelectron spectrum, but others are weak or absent. The discrepancy is not attributed to autoionization, but rather to selection rules governing the ejection of low energy electrons into high angular momentum waves.

B. Formation of C$_{60}^{++}$

This photoion yield curve is roughly linear at energies well above the threshold for C$_{60}^{++}$, but appears to have curvature near threshold. Due to this curvature, we are unable to resolve the discrepancy between two alternative values for the second ionization potential, but we favor the lower value.

C. Fragmentation of C$_{60}^{+}$

Fragmentation is only detected at the highest photon energy, 40.8 eV. A weak C$_{58}^{+}$ intensity and a marginal intensity at the C$_{56}^{+}$ mass are observed. These observations are consistent with earlier conclusions based on laser-vaporized C$_{60}^{+}$, which concluded that at least 19.2 eV of internal energy, and possibly as much as 39 eV was necessary to dissociate C$_{60}^{+}$. The lack of odd ionic fragments (e.g., C$_{57}^{+}$ + C$_3$) is attributed to their lower stability due to the fact that these do not form closed carbon cages, whereas the even numbered ones do. Manolopoulos et al.[34] have recently demonstrated a correlation between the *kinetic* stability of these species, as measured by their HOMO–LUMO gap, and the observed mass spectra.

The observed unimolecular decomposition of C$_{60}^{+}$ is consistent with quasiequilibrium theory, but more detailed experiments (e.g., photoion–photoelectron coincidence) and more precise models are required to convincingly demonstrate this point. Within the framework of the present experimental results and the model described, we favor a minimum energy for the dissociation process C$_{60}^{+} \rightarrow$ C$_{58}^{+}$ + C$_2$ of 6.0–6.5 eV, higher than the 4.6 eV previously deduced. In this model, the kinetic shift is in the neighborhood of 30 eV, whereas previously reported kinetic shifts for other molecules are of the order of tenths of an eV.

[1] W. Krätschmer, L. D. Lamb, K. Fostiropoulos, and D. R. Huffman, Nature 347, 354 (1990); See also, D. H. Parker, P. Wurz, K. Chatterjee, K. R. Lykke, J. E. Hunt, M. J. Pellin, J. C. Hemminger, D. M. Gruen, and L. M. Stock, J. Am. Chem. Soc. 113, 7499 (1991).

[2] S. C. O'Brien, J. R. Heath, R. F. Curt, and R. E. Smalley, J. Chem. Phys. 88, 220 (1988).

[3] M. E. Geusic, T. J. McIlrath, M. F. Jarrold, L. A. Bloomfield, R. R. Freeman, and N. L. Brown, J. Chem. Phys. 84, 2421 (1986); M. E. Geusic, M. F. Jarrold, T. J. McIlrath, R. R. Freeman, and W. L. Brown, ibid. 86, 3862 (1987). See also P. P. Radi, T. L. Bunn, P. R. Kemper, M. E. Molchan, and M. T. Bowers, ibid. 88, 2809 (1988).

[4] P. P. Radi, M.-T. Hsu, M. E. Rincon, P. R. Kemper, and M. T. Bowers, Chem. Phys. Lett. 174, 223 (1990).

[5] D. R. Luffer and K. H. Schramm, Rapid Commun. Mass Spectrom. 4, 552 (1990).

[6] A. B. Young, L. M. Cousins, and A. G. Harrison, Rapid Commun. Mass Spectrom. 5, 226 (1991).

[7] R. J. Doyle and M. M. Ross, J. Phys. Chem. 95, 4954 (1991).

[8] F. H. Dorman and J. D. Morrison, J. Chem. Phys. 35, 575 (1961).

[9] M. E. Wacks and V. H. Dibeler, J. Chem. Phys. 31, 1557 (1959).

[10] M. E. Wacks, J. Chem. Phys. 41, 1661 (1964).

[11] J. A. Zimmerman, J. R. Eyler, S. B. H. Bach, and S. W. McElvany, J. Chem. Phys. 94, 3556 (1991).

[12] D. L. Lichtenberger, K. W. Nebesny, C. D. Ray, D. R. Huffman, and L. D. Lamb, Chem. Phys. Lett. 176, 203 (1991).

[13] D. L. Lichtenberger, M. E. Jatcko, K. W. Nebesny, C. D. Ray, D. R. Huffman, and L. D. Lamb, Proc. Mater. Res. Soc. Symp. 206, 673 (1991).

[14] S. W. McElvany, M. M. Ross, and J. H. Callahan, Mater. Res. Soc. Symp. Proc. 206, 697 (1990); S. W. McElvany and S. B. H. Bach, Proceedings of the 39th Annual Conference, Am. Soc. Mass Spectrom. (1991), p. 422.

[15] C. Lifshitz, M. Iraqi, T. Peres, and J. E. Fischer, Rapid Commun. Mass Spectrom. 5, 238 (1991).

[16] A. Rosén and B. Wästberg, J. Chem. Phys. 90, 2525 (1989).

[17] U. von Barth and L. Hedin, J. Phys. C 5, 1629 (1972).

[18] R. B. Cairns and J. A. R. Samson, J. Opt. Soc. Am. 56, 1568 (1966).

[19] R. E. Stanton and M. D. Newton, J. Phys. Chem. 92, 2141 (1988).

[20] J. H. Weaver, J. L. Martins, T. Komeda, Y. Chen, T. R. Ohno, G. H. Kroll, N. Troullier, R. E. Haufler, and R. E. Smalley, Phys. Rev. Lett. 66, 1741 (1991).

[21] R. C. Haddon, L. E. Brus, and K. Raghavachari, Chem. Phys. Lett. 125, 459 (1986).

[22] E. E. B. Campbell, G. Ulmer, and I. V. Hertel, Phys. Rev. Lett. 67, 1986 (1991).

[23] E. P. Wigner, Phys. Rev. 73, 1002 (1948); G. H. Wannier, Phys. Rev. 90, 817 (1953); F. H. Read, in Electron Impact Ionization, edited by T. D. Märk and G. H. Dunn (Springer, New York, 1985), p. 49.

[24] D. M. Cox, S. Behal, M. Disko, S. M. Gorun, M. Greaney, C. S. Hsu, E. B. Kollin, J. Millar, J. Robbins, W. Robbins, R. D. Sherwood, and P. Tindall, J. Am. Chem. Soc. 113, 2940 (1991).

[25] P. M. Guyon and J. Berkowitz, J. Chem. Phys. 54, 1814 (1971).

[26] D. S. Bethune, G. Meijer, W. C. Tang, H. J. Rosen, W. G. Golden, H. Seki, C. A. Brown, and M. S. deVries, Chem. Phys. Lett. 179, 181 (1991).

[27] A precise value for the dissociation energy cannot be given, because of uncertainty in ΔH_f^0 (C$_4$H$_4^+$). H. M. Rosenstock, R. Stockbauer, and A. C. Parr, Int. J. Mass Spectrom. Ion Phys. 38, 323 (1981) give ΔH_{f0}^0 (C$_4$H$_4^+$) = 285.6 $\pm$ 2.9 kcal/mol, while J. H. D. Eland, J. Berkowitz, H. Schulte, and R. Frey, ibid. 28, 297 (1978) obtain a value between 277–282 kcal/mol. These values correspond to D_0 values for C$_6$H$_6^+ \rightarrow$ C$_4$H$_4$ + C$_2$H$_2$ of 4.48 $\pm$ 0.13 eV, or 4.20 $\pm$ 0.07 eV.

[28] S. W. Benson, Thermochemical Kinetics, 2nd ed. (Wiley, New York, 1976).

[29] W. Forst, Theory of Unimolecular Reactions (Academic, New York, 1973), p. 68.

[30] Ref. 29, p. 110. See also P. C. Haarhoff, Mol. Phys. 7, 901 (1963).

[31] T. Beyer and D. F. Swinehart, Commun. Assoc. Comput. Machin. 16, 372 (1973); S. E. Stein and B. S. Rabinovitch, J. Chem. Phys. 58, 2438 (1973).

[32] T. Baer, G. D. Willett, D. Smith, and J. S. Phillips, J. Chem. Phys. 70, 4076 (1979).

[33] D. Bakowics and W. Thiel, Chem. Phys. 151, 309 (1991).

[34] D. E. Manolopoulos, J. C. May, and S. E. Down, Chem. Phys. Lett. 181, 105 (1991).